Astronomy & Astrophysics manuscript no. Nicolas
December 19, 2019

Redshift evolution of the SN stretch distribution

N. Nicolas[1], M. Rigault[2], R. Graziani[2], M. Briday[1], Y. Copin[1], and Y. Kim[1]

[1] Université de Lyon, F-69622, Lyon, France; Université de Lyon 1, Villeurbanne; CNRS/IN2P3, Institut de Physique des Deux Infinis, Lyon
[2] Université Clermont Auvergne, CNRS/IN2P3, Laboratoire de Physique de Clermont, F-63000 Clermont-Ferrand, France.

Received 2 November 1992 / Accepted 7 January 1993

ABSTRACT

Context. Type Ia supernovae (SNe Ia) allow for the construction of the Hubble diagram, giving us information about the Universe's expansion and its fundamental components, one of which is dark energy. But systematic uncertainties are now starting to be limiting in our ability to measure those parameters. In particular, the physics of SNe Ia is still mostly unknown, and is thought not to change in time/with the redshift.
Aims. In an attempt to reduce those uncertainties, we try to find an empirical law describing SNe Ia's length of explosion (stretch) evolution with the redshift.
Methods. We started by getting a complete sample representing all of the stretch distribution that Nature can give us, before using LsSFR measurements, an age tracer which evolution with redshift is known, that has been shown to have a strong correlation with the stretch. We compare their AICc, an estimator of the relative quality of statistical models that includes the number of free parameters, to determine which ones describe best the data.
Results. Models with an evolution of the stretch with the redshift have a better AICc than the ones without.
Conclusions. We find that implementing these models allows us to fit the data better than models without stretch evolution.

Key words. Cosmology – Type Ia Supernova – Systematic uncertainties

1. Introduction

Type Ia supernovae (SNe Ia) are powerful cosmological distance indicators that have enabled the discovery of the acceleration of the Universe's expansion (Riess et al. 1998; Perlmutter et al. 1999). They remain today a key cosmological probe to understand the properties of dark energy (DE) as it is the only tool able to precisely map the recent expansion rate $z < 0.5$, when DE is driving it (e.g. Scolnic et al. 2019). They also are key to directly measure the Hubble Constant (H_0) provided one can calibrate their absolute magnitude (Riess et al. 2016; Freedman et al. 2019). Interestingly, the value of H_0 derived when the SNeIa are anchored on Cepheids (the SH0ES project Riess et al. 2009, 2016) is $\sim 5\ \sigma$ higher than what is predicted by cosmic microwave background (CMB) data measured by Planck assuming the standard ΛCDM or when the SN luminosity is anchored at intermediate redshift by the baryon acoustic oscillation (BAO) scale (Riess et al. 2019; Reid et al. 2019; Planck Collaboration et al. 2016; **?**) changed ried to reid; changed planck to planck2016; feeney = https://tinyurl.com/vg6uufm ?. While using the tip of the red giant branch technique in place of the Cepheids seem to favor lower values of H_0 (Freedman et al. 2019; **?**) changed "freedman" to "freedman2019" ; recalibrationpaper = ? time delay measurements from strong lensing seem to also favor high H_0 values (Wong et al. 2019).

The H_0 tension has received a lot of attention as it could be a sign of new fundamental physics. Yet, no simple solution is able to accommodate this H_0 tension when accounting for all other probes and the current most promising scenario appears to be a burst of expansion at the matter-radiation decoupling moment caused by a (fine tuned) early dark energy (Poulin et al. 2019) changed "poulin" to "poulin 2019".

Alternatively, systematic effects affecting one or several of the aforementioned analysis could also explain the tension. In Rigault et al. (2015) we suggested that SNe Ia from the Cepheid calibrator sample differ significantly to the one from the Hubble flow sample that enables to derive H_0. Indeed, Cepheid are very young stars and the existence of Cepheids in a galaxy implies that the host is star forming. In (Rigault et al. 2015) we claimed that a more than 90% of the calibrator SNe Ia arise from a young-progenitor population while this population only accounts for about half of the Hubble flow sample. Following Sullivan et al. (2010) and (Rigault et al. 2013) should use cite or citep?, we further showed that young and old progenitor SNe Ia have a different magnitude of about 0.15 mag. This has been confirmed for modern standardization technique (SALT2.4 Guy et al. 2010; Betoule et al. 2014) with high significance ($\sim 6\sigma$) in (Rigault et al. 2018) as well as independently by **?** not found on ADS: https://tinyurl.com/uematttg at $\sim 7\sigma$. As detailed in (Rigault et al. 2015), if the magnitude difference between young and old SNe Ia is indeed of 0.15 mag and if SNe Ia from the calibrator sample is fully dominated by young SNeIa, the effect on H_0 of the existence of these two SNe Ia populations is of 3.5%. Accounting for the fact that another environmental effect (the mass-step) is already included in the SH0ES analysis, the net bias in the SH0ES analysis is expected closer to 3% (see table 6 of Rigault et al. 2015).

SHOULD BE SHORTENED A LOT: However, the importance of this astrophysical bias in the direct measurement of H_0 is still highly debated. We also highlight that it could not explain the high value of H_0 derived by strong lensing. First, Jones et al. (2015) put the ref but nos sure it's the correct one did not find any environmental bias when extending the (Rigault et al. 2015) study. It was more recently reported in (Jones et al. 2019) put the

ref but nos sure it's the correct one that indeed local host analysis has significant influence on the SN magnitude but much more importantly than claimed in (Rigault et al. 2018) and with a connection with the progenitor physics and/or a line of sight effect that is unclear. More importantly, Riess et al. (2016) attended to mimic the Cepheid sample selection function on the Hubble flow sample by removing SNe Ia from the latter if they classified their host as early-type or non-star forming. They measured that doing so has no effect on the measurement of H_0.

This paper is part of a series of papers where we test the validity of the two SNe Ia population models developed in (Rigault et al. 2018).Briday et al. in prep will present how using different environmental tracer is affecting our ability to distinguish the two populations, and Rigault et al. in prep will further study the connection with H_0. Here we analyze predictions concerning the SNe Ia redshift drifts: (1) that the distribution of the SNIa stretch, a purely intrinsic SNIa property, is evolving as a function of redshift and (2) that this population-drift follows the relation that (Rigault et al. 2018) derived assuming that one population is "young" with a rate proportional to the star formation rate in the Universe and the second is "old" with a rate proportional to the stellar mass.

The concept of the SNeIa age dichotomy arised when the SNIa rate has first been studied. Mannucci et al. (2005); Scannapieco & Bildsten (2005); Sullivan et al. (2006); Aubourg et al. (2008) have shown that the relative SNe Ia rate in galaxies could only be explained if two populations existed, one young, following the host star formation activity, and one old following the host stellar mass (the so called "prompt and delayed" or "A+B" model). In Rigault et al. (2018) we used the specific star formation rate at the SN location (Local sSFR or LsSFR) to classify which are the prompts (those with a high LsSFR) and which are the delayed (those with low LsSFR). Since the first SNe Ia host analysis, the SN stretch has been known to be strongly correlated with the SN host properties (Hamuy et al. 1996, 2000) put hamuy1996 as most cited of https://tinyurl.com/sjlbdz8 and it has been extensively confirmed since (e.g. Neill et al. 2009; Sullivan et al. 2010; Lampeitl et al. 2010; Kelly et al. 2010; Gupta et al. 2011; D'Andrea et al. 2011; Childress et al. 2013; Rigault et al. 2013; Pan et al. 2014) added all the refs. Following the "A+B" model and the connection between SN stretch and host properties, (Howell et al. 2009) changed howell20xx to howell2009 (https://ui.adsabs.harvard.edu/abs/2009ApJ...691..661H/abstract) first discussed the potential redshift drift of the SN stretch distribution. In this paper we revisit this analysis with the most recent SNe Ia dataset and we test the validity of the two SNIa age populations model developed by (Rigault et al. 2018).

We present in section 2 the sample we are using for this analysis, which is based on the pantheon dataset (Scolnic et al. 2018). We discuss the importance of obtaining a "complete" sample, i.e. representative of the true underlying SNe Ia distribution, and how we build one from the Pantheon sample. We then present in section 3 our modeling of the distribution of stretch as a function of redshift based on the relative stretch distribution of young and old SNeIa. Our results are presented in section 4 where we test if the distribution of stretch does evolve as a function of redshift and if the age-model is in good agreement with this evolution. We discuss our results and conclude in section 6.

Throughout the paper we use the Planck 2015 cosmology from the astropy library.

2. A "complete" Sample

We base our analysis on the latest SNe Ia compilation: the Pantheon catalog from Scolnic et al. (2018). TO BE REPHRASED Using this dataset, we aim at probing if the average stretch, an intrinsic SN Ia property, evolves as a function of redshift or not; the underlying question being that of the SNIa population redshift drift. The stretch has been shown to depend on the SN environment star formation activity (e.g. Howell et al. 2007; Sullivan et al. 2010; Childress et al. 2013; Rigault et al. 2013; Rigault et al. 2018) and because the star formation rate is about 40 times larger at the high redshift end of the pantheon sample than at its lower redshifts (e.g., Tasca et al. 2015, and references therein), one might think that simply comparing the redshifts distribution in a few bins of redshift could be sufficient to probe any SN stretch redshift drift. In practice, selection effects are affecting the observed SN stretch distributions, which could significantly differ from the true underlying one if these selection effects become significant. Indeed, because the observed SNIa magnitude correlates with the lightcurve stretches (and colors) the first SNIa that such a survey will miss will the reddest and the lowest-stretch ones. Consequently, if selection effects is not accounted for, one might confuse true population drift with selection effect and conversely.

In a magnitude limited survey, providing sufficient (and random) spectroscopic follow-up for acquiring typing and host redshift, the selection effects should be negligible bellow a given redshift where all SNe Ia, even the faintest, could be observed. In contrast, targeted surveys have highly complex selection functions and we will discard them from our analysis. Fortunately, modern SN cosmology sample such has the pantheon dataset are now dominated by magnitude limited survey.

We present fig. 1 the lightcurve stretch and color distributions of SNeIa from these surveys, namely: PanStarrs (PS1 **?**), the Sloan Digital Sky Survey (SDSS **?**) and the SuperNovae Legacy Survey (SNLS Astier et al. 2006). An ellipse in the salt2.4 (x_1, c) plan with major axis $x_1 = 3$ and manor axis $c = 0.3$ encapsulates the full distribution (see also Bazin et al. 2011 and Campbell et al. 2013 for a similar contour but using a less conservative $c = 0.2$ for the latter). Assuming the SN absolute magnitude with $x_1 = 0$ and $c = 0$ is $M = -19.36$ (Kessler et al. 2009; Scolnic et al. 2014) we can derive the absolute standardized magnitude at maximum of light along the aforementioned ellipse given the standardization coefficient $\alpha = 0.16$ and $\beta = 3.14$ from Scolnic et al. (2018). The faintest SNIa is that with $x_1 = -1.66$ and $c = 0.25$ and has an absolute standardized magnitude at peak in Bessel-b band of -18.31 mag. Since we need to see this object typically a week before and 10 days after peak to build a suitable lightcurve, the effective absolute limiting magnitude therefore is ~ -18.00 mag. Hence, given the 5σ point source detection magnitude limit of a magnitude limited survey, one can derive the maximum redshift above which the faintest SNeIa will start to be missed.

SNLS typically acquires SNeIa in the redshift range $0.4 < z < 0.8$. At these redshifts the rest-frame Bessel-b band roughly corresponds to the SNLS-i filter that has a 24.8 mag 5σ depth[1]. This converts to a $z_{lim} = 0.60$, in perfect agreement with Neill et al. (2006), Perrett et al. (2010) and Bazin et al. (2011). Similarly, PS1 observes SNeIa in the range $0.2 < z < 0.4$, their g-band 5σ depth is 23.1 mag (Rest et al. 2014), which yields to $z_{lim} = 0.30$. Figure 6 of (Scolnic et al. 2018) suggests a more conservative z_{lim} of 0.27 for the PS1 catalog. In similar redshift range, SDSS has a limiting magnitude of 22.5 (Dilday et al. 2008; Sako et al.

[1] CFHT final release website.

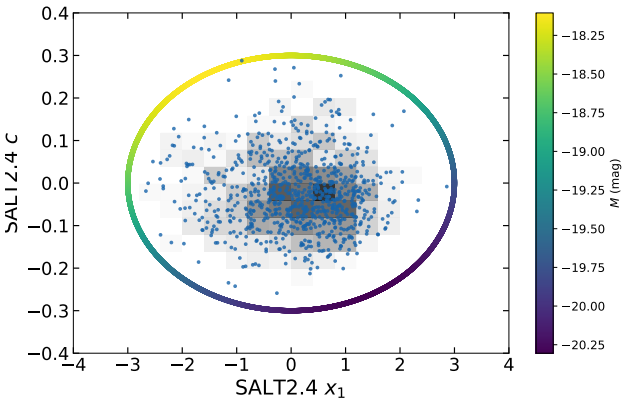

Fig. 1. SALT2.4 stretch and color lightcurve parameters of SNeIa from the SDSS, PS1 and SNLS samples from the pantheon catalog. The individual SN data are shown as blue dots and a 2D histogram is shown in gray to highlight point density. The ellipse encapsulating all the SN data is displayed colored by the effective standardized absolute magnitude using the α and β standardization coefficients from (Scolnic et al. 2018).

Table 1. Source surveys of SNeIa used in our "complete" sample. Conservative cuts are indicated in brackets.

Survey	N_{SN}	z_{max}
SNf	114	–
SDSS	167(82)	0.20(0.15)
PS1	160(122)	0.30(0.27)
SNLS	102(78)	0.60(0.55)
HST	26	–

2008), which would lead to a $z_{lim} = 0.24$. However, the SDSS survey were more sensitive to limited spectroscopic resources. Kessler et al. (2009) present that during year-1 of SDSS, SNeIa with $r - mag < 20.5$ were favored for spectroscopic follow up, corresponding to the redshift cut at 0.15. For the rest of the SDSS survey, additional spectroscopic resources were used, such that Kessler et al. (2009) and Dilday et al. (2008) show a relative completeness up to $z_{lim} = 0.2$. Following these analysis we will use $z_{lim} = 0.2$ as the baseline SDSS redshift limit for the rest of the analysis. We could have chosen more conservative redshift limits for each of these surveys, namely $z_{lim} = 0.15$ for SDSS, $z_{lim} = 0.27$ for PS and $z_{lim} = 0.55$ for SNLS, following Fig. 14 of Perrett et al. 2010, and we will also present results obtained when doing so. We present the redshift distribution of these three surveys in fig. 2, where we see that the redshift limit roughly correspond to the pick of these histograms, as expected.

In addition, we use the SNeIa from the nearby supernovae factory (SNfactory Aldering 2004) added ref assuming https://ui.adsabs.harvard.edu/abs/2004APS..APR.V4003A/abstract published in (Rigault et al. 2018) and that have been discoverd from no-targeted survey (114 SNeIa, see their section 3 and 4.2.2). As the SNe search were much deeper than the spectrophotometric follow-up, SNfactory SNe Ia within a redshift range of $0.02 < z < 0.09$ should also be a random sampling of the underlying SN population. Data from (Rigault et al. 2018) are within these redshift boundaries. The HST sample from Pantheon follows the same logic and we therefore kept it entirely (**?**) lots of choices: https://tinyurl.com/rcsx7cw.

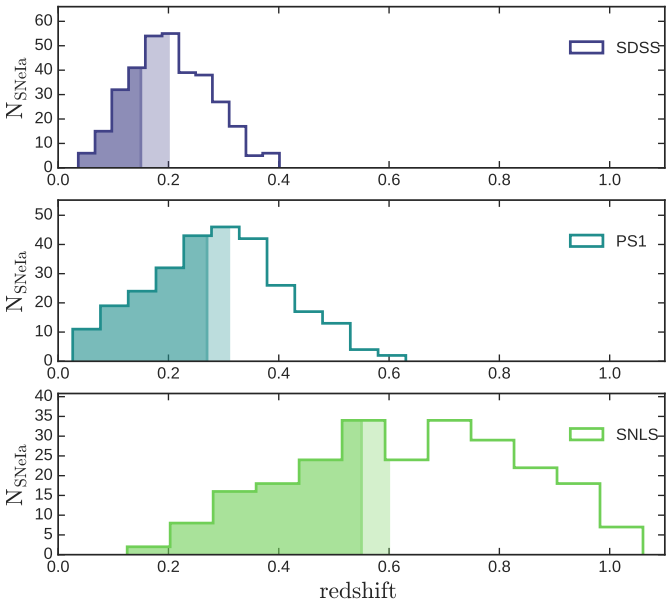

Fig. 2. Histograms of the 3 surveys on which we applied cuts to get rid of selection effects, as discussed in section 2. The SNe Ia between the conservative and non-conservative cuts are shown in transparent.

3. Modeling the redshift drift

In Rigault et al. (2018) we presented a modeling of the evolution of the fraction of prompt and delayed SNeIa as a function of redshift following former work on rates and delay time distributions; see e.g. the prompt and delayed SNeIa model, aka the "A+B" model, Mannucci et al. (2005); Scannapieco & Bildsten (2005); Sullivan et al. (2006); Aubourg et al. (2008) and Maoz et al. (2014) for a review on delay time distributions of SNeIa. In short, we assume that the number of prompt SNeIa follows the star formation activity in the Universe while the number of delayed SNeIa follows the number of Gyr-old stars in the Universe, i.e. the stellar mass. Hence, if we denote calling $\delta(z)$ (resp. $\phi(z)$) the fraction of young (resp. old) SNeIa in the Universe as a function of redshift, then their ratio is expected to follow the evolution of the specific star formation rate which goes as $(1+z)^{2.8}$ until $z \sim 2$ (Tasca et al. 2015). Hence since there is $\sim 50\%$ of young SNeIa at $z \sim 0.05$ (Rigault et al. 2013; Rigault et al. 2018), in agreement with rate expectations (Mannucci et al. 2006; Rodney et al. 2014), then, we find in Rigault et al. (2018):

$$\delta(z) = \left(K^{-1} \times (1+z)^{-2.8} + 1\right)^{-1} \text{ or,} \quad (1)$$

$$\psi(z) = \left(K \times (1+z)^{+2.8} + 1\right)^{-1}, \quad (2)$$

where $K = 0.87$ given the fraction of young in the SNfactory sample. This modelisation is comparable to the evolution predicted by Childress et al. (2014) based on SN rates in galaxies depending on their quenching time as a function of their stellar mass.

3.1. With LsSFR data

In Rigault et al. (2018) we present that the SN stretch is strongly correlated with the LsSFR, which traces age. We present this correlation in fig. 3.1. To model the evolution of the SN stretch as a function of redshift given our aforementioned model of the evolution of the fraction of young (old) SNeIa, we need to model

the SN stretch distribution of each age sample. Given the structure of the stretch–LsSFR scatter plot show fig. 3.1, we define our model as follows: for the young population the underlying stretch distribution is modeled as $\mathcal{N}(\mu_1, \sigma_1)$, i.e. a normal distribution centered on μ_1 with a σ_1 width ; the old population stretch distribution is modeled as $a \times \mathcal{N}(\mu_1, \sigma_1) + (1-a) \times \mathcal{N}(\mu_2, \sigma_2)$, i.e. a gaussian mixture where one mode is the same as the young population one. The estimation of the 5 free parameters ($\theta \equiv \mu_1, \mu_2, \sigma_1, \sigma_2, a$) of the model is given by minimizing:

$$\mathcal{L} = -2 \sum_i \ln\left(\mathcal{P}\left(x_1^i \mid \theta\,; \mathrm{d}x_1^i, p(y)^i\right)\right), \tag{3}$$

with

$$\begin{aligned}\mathcal{P}\left(x_1^i \mid \theta\,; \mathrm{d}x_1^i, p(y)^i\right) = p(y)^i \times \mathcal{N}\left(\mu_1, \sqrt{{\sigma_1}^2 + {\mathrm{d}x_1^i}^2}\right)(x_1^i) + \\ (1-p(y)^i) \times [a \times \mathcal{N}\left(\mu_1, \sqrt{{\sigma_1}^2 + {\mathrm{d}x_1^i}^2}\right)(x_1^i) + \\ (1-a) \times \mathcal{N}\left(\mu_2, \sqrt{{\sigma_2}^2 + {\mathrm{d}x_1^i}^2}\right)(x_1^i)\,],\end{aligned} \tag{4}$$

where i is the index of the SNIa, x_1^i, $\mathrm{d}x_1^i$ and $p(y)^i$ are the salt2.4 stretch, error of the salt2.4 stretch and the probability that the SN is prompt, respectively. In practice, since "a" is defined between 0 and 1, we fit for α such that $a = \arctan(\alpha)/\pi + 0.5$, which results into asymmetric error on a.

The fit results are shown table 2 and the best fit model is illustrated in fig. 3.1.

When combining our prediction of the evolution of young SNeIa as a function of redshift eq. 1, and the stretch distribution of the both the young and the old SNeIa, our model for the underlying distribution of stretch $\Delta(x_1|z)$ as a function of redshift is:

$$\begin{aligned}\Delta(x_1 \mid z) = \delta(z) \times \mathcal{N}(\mu_1, \sigma_1) + \\ (1-\delta(z)) \times [a \times \mathcal{N}(\mu_1, \sigma_1) + (1-a) \times \mathcal{N}(\mu_2, \sigma_2)]\end{aligned} \tag{5}$$

3.2. Without LsSFR data

Given eq. 5, we can extend the analysis by fitting the free parameters of the model ($\theta \equiv \mu_1, \mu_2, \sigma_1, \sigma_2, a$) assuming the evolution of the fraction of young SNeIa as a function of redshift given by $\delta(z)$ and given, this time, x_1^i, $\mathrm{d}x_1^i$ and z^i, the stretch, error on the stretch and redshift of any given SN i. In practice, it means that we are still minimizing for the same eq. 3, but replacing $p(y)^i$ by $\delta(z^i)$ eq. 4.

The fit results when using the conservative redshift cuts or not are shown table 2 and the best fit models are illustrated in fig. 4.

3.3. Other modelings

In section 3.1 and 3.2 we have modeled the underlying stretch distribution as a single gaussian for the young SNe Ia and a combination of two gaussians for the old SNe Ia population, i.e., the same as the young-population one plus another for the fast declining SNeIa that seem to only exist in old populations.

Howell et al. (2007) used a simpler modelisation: the underlying stretch of each age population is a single gaussian. This rises the question of the accuracy of our modeling choice. To test this, we have implemented a suite of extra parametrisation that we also fit to the data following the procedure described section 3.2. Namely we consider:

- "Base+(μ_1^O, σ_1^O)": base model but where the high-stretch Gaussian of the old population is not set as that of the young population ;
- "Base−(σ_2)": base model but where σ_2 is fixed at the same value as σ_1, since both width seem not significantly different in Table 2;
- "Howell": one single Gaussian per age group as in (Howell et al. 2007), but with the $\delta(z)$ factor.

Furthermore, since we aim at probing the SN redshift drift, we are also fitting the "Base" model and the three aforementioned extensions by fixing the population drift parameter $\delta(z)$ to a free parameter constant $\delta(z) = f$. Doing so enables us to consider two last models. The first is modeling the underlying SNe Ia stretch distribution by a simple Gaussian, namely "Gaussian (f)". The second is using an asymmetric Gaussian distribution as currently done by the BBC formalism introduced by Kessler, & Scolnic (2017); Scolnic et al. (2018) for modeling the sample selection functions in SN Cosmology. This last model is particularly interesting to test as it is currently used in the most recent SN Cosmological analyses Riess et al. (2016, 2018); **?**); Scolnic et al. (2018); **?** supposed riess2018 to be https://ui.adsabs.harvard.edu/abs/2018ApJ...861..126R/abstract; see further discussion concerning this issue in section 5.1.

The ability of the model to explain the data is detailed in section 4.

4. Results

We applied each model on both the conservative and non-conservative sample (cf. section 2. We want to test whether including an evolution of the stretch with the redshift ($\delta(z)$ factor) would better describe the data. As the various models presented section 3, have various degrees of freedom. To compare them all, we use the Akaike Information Criterion corrected for sample size (AICc), that penalizes extra degrees of freedom to avoid over-fitting the data. The AICc is defined as follow:

$$\mathrm{AICc} = \mathrm{AIC} + \frac{2k(k+1)}{n-k-1} \tag{6}$$

with $\mathrm{AIC} = 2k + \mathcal{L}$, where k is the number of free parameters and $\mathcal{L}$ is defined eq (3). The best model is the one with the smaller AICc and the probability for another model to be at least as representative of the data as this one is given by:

$$p(\mathrm{other} > \mathrm{best}) = \exp(\Delta\mathrm{AICc}/2) \tag{7}$$

The results are summarized in table 3 and represented figure 5.

For the non-conservative part, we find that every model lacking an evolution of the stretch with the redshift is systematically worse than those that implement it, and that removing the σ_2 parameter gives better results than letting it free, or adding (μ_1^O, σ_1^O). However, the base model with 2 gaussians for the old population is roughly the same as the Howell model with one gaussian per population. As for the conservative part, all the models but the asymmetric and the gaussian ones correctly fit the data. No fixed model fit better than those with evolution, but some come close. It would seem that taking SNe Ia close to us doesn't give us a sample where the evolution is visible, justifying the study done in section 2.

5. discussion

5.1. BBC and assumptions on underlying SN property

BBC use the asymmetric model. When we do it, we get the table TABLE

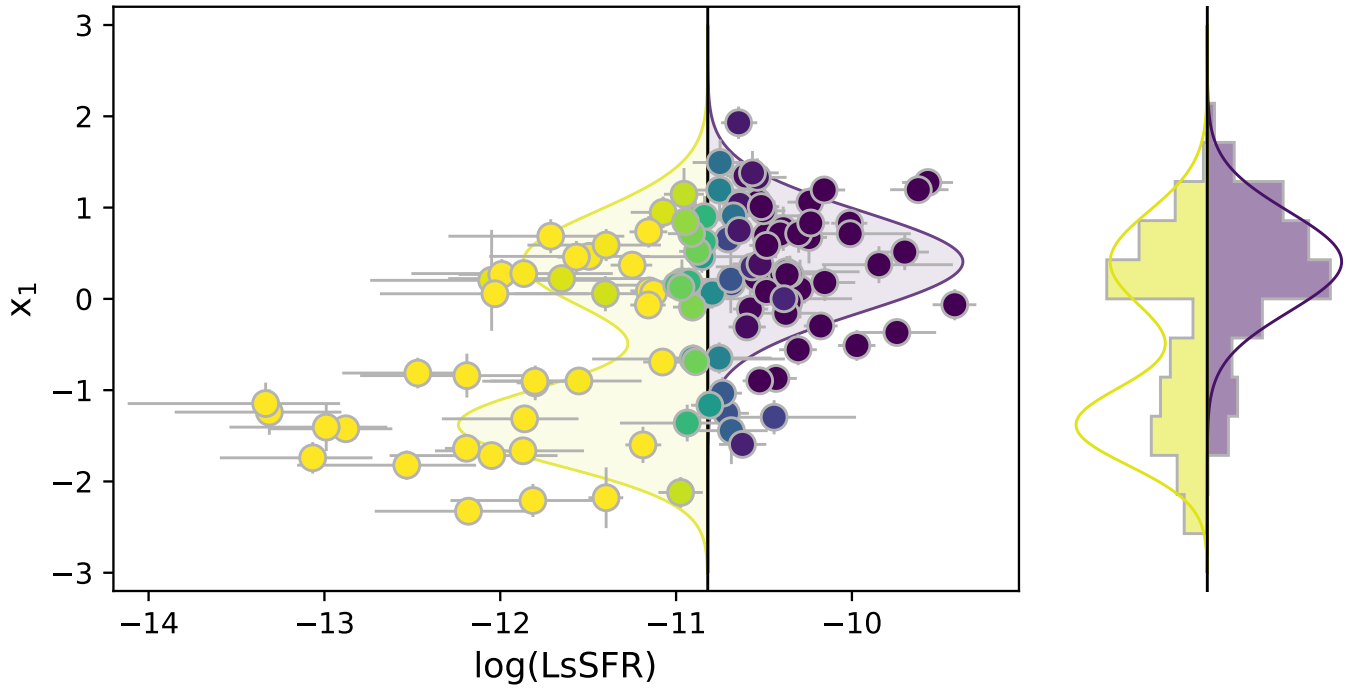

Fig. 3. SNF data on which we based our models of stretch distribution between young and old

Table 2. Best fit value of the stretch distribution model. The "SNf" results are derived using eq. 4 solely using the SNf data for which we have $p(y)$. The "All" and "All(cons)" results are derived using eq. 3 without the age information (see section 3.2) ; "All(cons)" correspond to the "complete sample" using conservative redshift cut (see section 2).

Sample	μ_1	σ_1	μ_2	σ_2	a
SNf	0.41 ± 0.08	0.55 ± 0.06	-1.38 ± 0.10	0.44 ± 0.08	$0.48^{+0.08}_{-0.08}$
All	0.43 ± 0.09	0.58 ± 0.05	-1.05 ± 0.28	0.63 ± 0.13	$0.51^{+0.09}_{-0.10}$
All(cons)	0.38 ± 0.05	0.60 ± 0.06	-1.26 ± 0.13	0.53 ± 0.08	$0.47^{+0.09}_{-0.08}$

Table 3. Comparison of quality of fit for all the models. Base indicates the models designed for this study. (F) indicates models without an evolution of the fraction of young SNe Ia as a function of the redshift.

			All SNeIa (569)				All SNeIa (conservative ; 422)			
Name	drift(?)	Free param	$\ln \mathcal{L}$	AICc	ΔAICc	Proba	$\ln \mathcal{L}$	AICc	ΔAICc	Proba
Base$-(\sigma_2)$	$\delta(z)$	4	1456.9	1464.9	–	–	1079.9	1088.0	–	–
Base	$\delta(z)$	5	1456.7	1466.8	-1.8	4.0×10^{-1}	1079.5	1089.6	-1.7	4.4×10^{-1}
Base$+(\mu_1^O, \sigma_1^O)$	$\delta(z)$	7	1453.1	1467.3	-2.4	3.1×10^{-1}	1074.5	1088.8	-0.8	6.7×10^{-1}
Howell	$\delta(z)$	4	1463.3	1471.3	-6.4	4.1×10^{-2}	1088.2	1096.3	-8.3	1.5×10^{-2}
Assymetric	f	3	1485.2	1491.3	-26.3	1.9×10^{-6}	1101.3	1107.4	-19.4	6.2×10^{-5}
Howell	f	5	1484.2	1494.3	-29.4	4.2×10^{-7}	1101.2	1111.3	-23.4	8.5×10^{-6}
Base$+(\mu_1^O, \sigma_1^O)$	f	8	1478.9	1495.2	-30.2	2.8×10^{-7}	1095.5	1111.9	-23.9	6.5×10^{-6}
Base	f	6	1484.2	1496.4	-31.4	1.5×10^{-7}	1101.2	1113.4	-25.4	3.0×10^{-6}
Gaussian	–	2	1521.8	1525.8	-60.9	6.0×10^{-14}	1142.6	1146.6	-58.6	1.9×10^{-13}
Base$-(\sigma_2)$	f	5	1521.8	1531.9	-67.0	2.9×10^{-15}	1142.6	1152.7	-64.7	8.8×10^{-15}

6. Conclusion

Stretch evolution with the redshift is a thing. Need to see if it has an impact on the cosmology though.

Acknowledgements. This project has received funding from the European Research Council (ERC) under the European Union's Horizon 2020 research and innovation programme (grant agreement n 759194 - USNAC).

References

Abbott, T. M. C., Abdalla, F. B., Alarcon, A., et al. 2018, Phys. Rev. D, 98, 043526
Aldering, G. 2004, APS April Meeting Abstracts 2004, V4.003
Astier, P., Guy, J., Regnault, N., et al. 2006, A&A, 447, 31
Ata, M., Kitaura, F.-S., Chuang, C.-H., et al. 2017, MNRAS, 467, 3993
Aubourg, É., Tojeiro, R., Jimenez, R., et al. 2008, A&A, 492, 631
Betoule, M., Kessler, R., Guy, J., et al. 2014, A&A, 568, A22

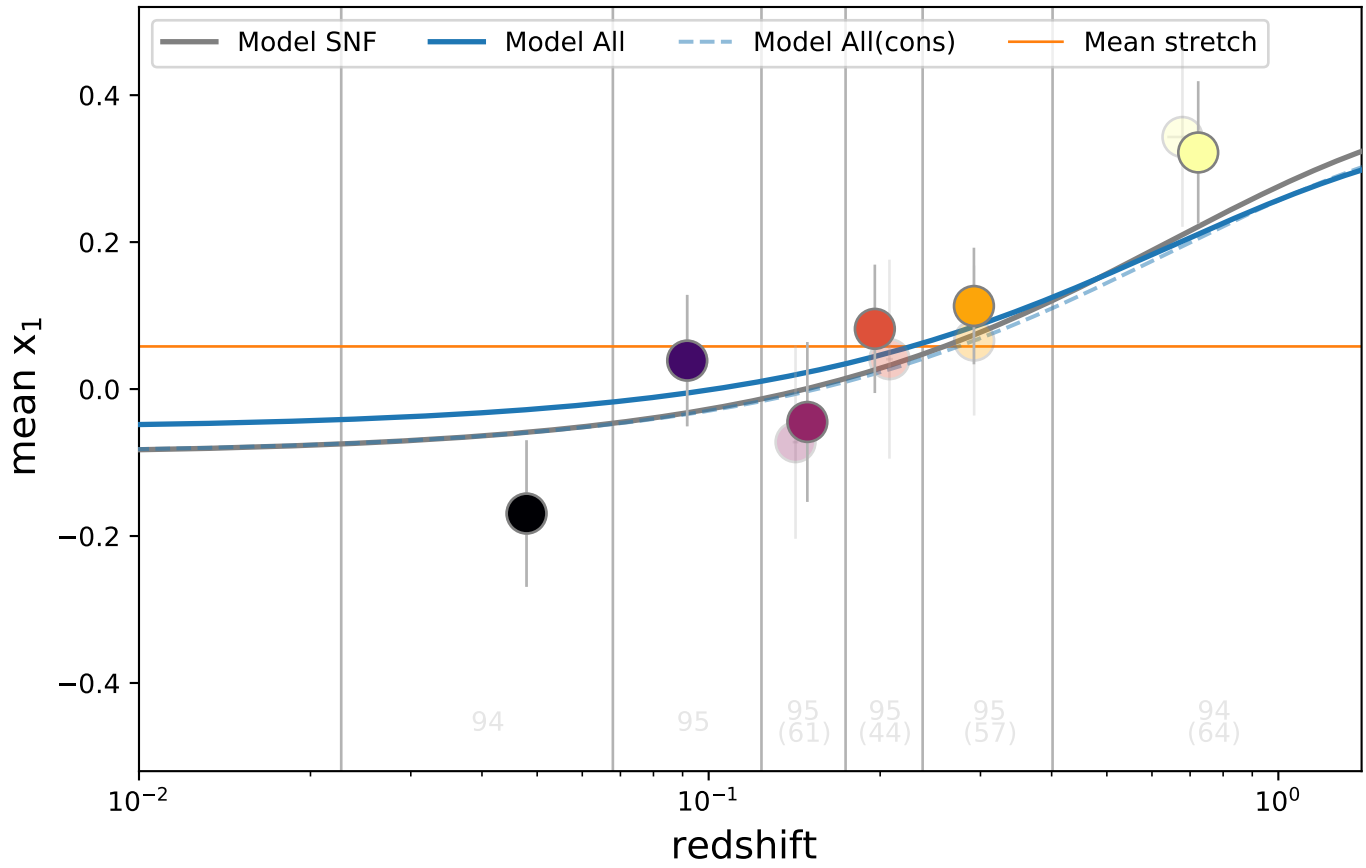

Fig. 4. Result of the model fitted on all the surveys' data, cut at the conservative $z_{\max}$ in transparent and non-conservative $z_{\max}$ in full markers. The number of SNe Ia in each bin is indicated just above the x-axis in transparent text; between brackets are the numbers for the conservative cuts.

Table 4. Fit results of the asymmetric and base models for the 3 surveys having selection effects.

Asymetric	Free param	σ^-	$\sigma^-_{\rm err}$	σ^+	$\sigma^+_{\rm err}$	μ^0	$\mu^0_{\rm err}$	ln $\mathcal{L}$	AICc
SDSS	3	1.25	0.08	0.39	0.07	0.69	0.10	893.9	900.0
PS1	3	1.00	0.09	0.49	0.09	0.42	0.12	702.0	708.1
SNLS	3	1.18	0.11	0.39	0.11	0.81	0.15	594.8	600.9
Total	9	–	–	–	–	–	–	2190.7	2209.0

Base	Free param	ln $\mathcal{L}$	AICc
SDSS	0	395.2	405.6
PS1	0	444.7	455.0
SNLS	0	254.1	264.7
Total	0	1094.0	1125.4

Bazin, G., Ruhlmann-Kleider, V., Palanque-Delabrouille, N., et al. 2011, A&A, 534, A43
Campbell, H., D'Andrea, C. B., Nichol, R. C., et al. 2013, ApJ, 763, 88
Chabanier, S., Millea, M., & Palanque-Delabrouille, N. 2019, MNRAS, 489, 2247
Childress, M., Aldering, G., Antilogus, P., et al. 2013, ApJ, 770, 108
Childress, M. J., Wolf, C., & Zahid, H. J. 2014, MNRAS, 445, 1898
Coles, P., & Jones, B. 1991, MNRAS, 248, 1
D'Andrea, C. B., Gupta, R. R., Sako, M., et al. 2011, ApJ, 743, 172
Dilday, B., Kessler, R., Frieman, J. A., et al. 2008, ApJ, 682, 262
Freedman, W. L., Madore, B. F., Hatt, D., et al. 2019, ApJ, 882, 34
Gupta, R. R., D'Andrea, C. B., Sako, M., et al. 2011, ApJ, 740, 92
Guy, J., Sullivan, M., Conley, A., et al. 2010, A&A, 523, A7
Hamuy, M., Phillips, M. M., Suntzeff, N. B., et al. 1996, AJ, 112, 2391
Hamuy, M., Trager, S. C., Pinto, P. A., et al. 2000, AJ, 120, 1479
Howell, D. A., Sullivan, M., Conley, A., et al. 2007, ApJ, 667, L37
Howell, D. A., Sullivan, M., Brown, E. F., et al. 2009, ApJ, 691, 661
Jones, D. O., Riess, A. G., & Scolnic, D. M. 2015, ApJ, 812, 31
Jones, D. O., Riess, A. G., Scolnic, D. M., et al. 2018, ApJ, 867, 108
Jones, D. O., Scolnic, D. M., Foley, R. J., et al. 2019, ApJ, 881, 19
Kelly, P. L., Hicken, M., Burke, D. L., et al. 2010, ApJ, 715, 743
Kessler, R., Becker, A. C., Cinabro, D., et al. 2009, ApJS, 185, 32
Kessler, R., & Scolnic, D. 2017, ApJ, 836, 56
Knox, L., & Millea, M. 2019, arXiv e-prints, arXiv:1908.03663
Lampeitl, H., Smith, M., Nichol, R. C., et al. 2010, ApJ, 722, 566
Mannucci, F., Della Valle, M., Panagia, N., et al. 2005, A&A, 433, 807
Mannucci, F., Della Valle, M., & Panagia, N. 2006, MNRAS, 370, 773
Maoz, D., Mannucci, F., & Nelemans, G. 2014, ARA&A, 52, 107
Neill, J. D., Sullivan, M., Balam, D., et al. 2006, AJ, 132, 1126
Neill, J. D., Sullivan, M., Howell, D. A., et al. 2009, ApJ, 707, 1449
Pan, Y.-C., Sullivan, M., Maguire, K., et al. 2014, MNRAS, 438, 1391
Perlmutter, S., Aldering, G., Goldhaber, G., et al. 1999, ApJ, 517, 565
Perrett, K., Balam, D., Sullivan, M., et al. 2010, AJ, 140, 518
Planck Collaboration, Ade, P. A. R., Aghanim, N., et al. 2016, A&A, 594, A13

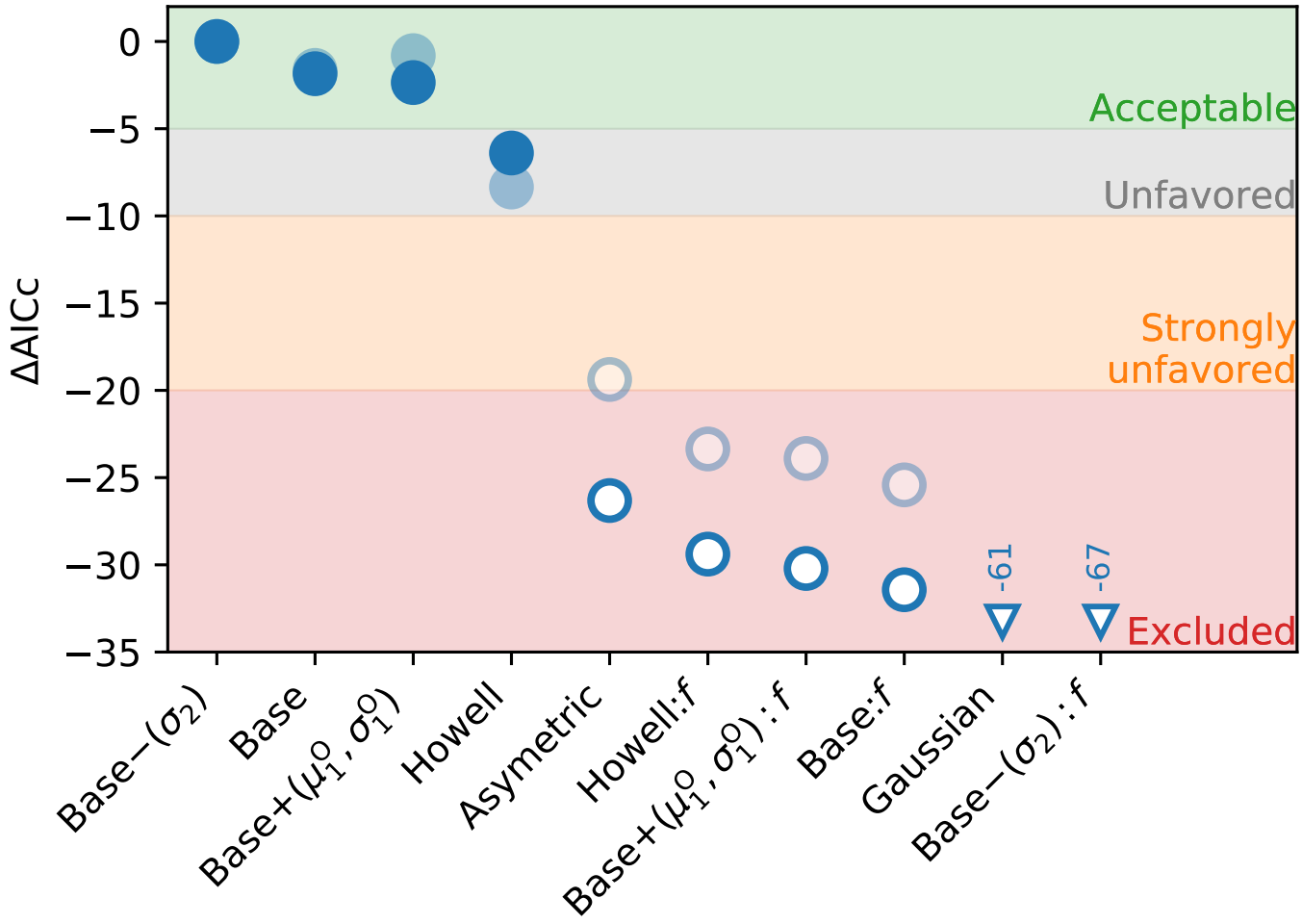

Fig. 5. ΔAICc of the models fitted on all the surveys' data, cut at the conservative z_{max} in transparent and non-conservative z_{max} in full markers.

Poulin, V., Smith, T. L., Karwal, T., et al. 2019, Phys. Rev. Lett., 122, 221301
Planck Collaboration, Aghanim, N., Akrami, Y., et al. 2018, arXiv e-prints, arXiv:1807.06209
Reid, M. J., Pesce, D. W., & Riess, A. G. 2019, arXiv e-prints, arXiv:1908.05625
Rest, A., Scolnic, D., Foley, R. J., et al. 2014, ApJ, 795, 44
Riess, A. G., Filippenko, A. V., Challis, P., et al. 1998, AJ, 116, 1009
Riess, A. G., Macri, L., Casertano, S., et al. 2009, ApJ, 699, 539
Riess, A. G., Macri, L. M., Hoffmann, S. L., et al. 2016, ApJ, 826, 56
Riess, A. G., Casertano, S., Yuan, W., et al. 2018, ApJ, 861, 126
Riess, A. G., Casertano, S., Yuan, W., et al. 2019, ApJ, 876, 85
Rigault, M., Copin, Y., Aldering, G., et al. 2013, A&A, 560, A66
Rigault, M., Aldering, G., Kowalski, M., et al. 2015, ApJ, 802, 20
Rigault, M., Brinnel, V., Aldering, G., et al. 2018, arXiv:1806.03849
Rodney, S. A., Riess, A. G., Strolger, L.-G., et al. 2014, AJ, 148, 13
Sako, M., Bassett, B., Becker, A., et al. 2008, AJ, 135, 348
Scannapieco, E., & Bildsten, L. 2005, ApJ, 629, L85
Scolnic, D., Rest, A., Riess, A., et al. 2014, ApJ, 795, 45
Scolnic, D. M., Jones, D. O., Rest, A., et al. 2018a, ApJ, 859, 101
Scolnic, D. M., Lochner, M., Gris, P., et al. 2018, arXiv e-prints, arXiv:1812.00516
Scolnic, D., Perlmutter, S., Aldering, G., et al. 2019, Astro2020: Decadal Survey on Astronomy and Astrophysics, 2020, 270
Sullivan, M., Le Borgne, D., Pritchet, C. J., et al. 2006, ApJ, 648, 868
Sullivan, M., Conley, A., Howell, D. A., et al. 2010, MNRAS, 406, 782
Tasca, L. A. M., Le Fèvre, O., Hathi, N. P., et al. 2015, A&A, 581, A54
Wong, K. C., Suyu, S. H., Chen, G. C.-F., et al. 2019, arXiv e-prints, arXiv:1907.04869
Z